Effect of carbon incorporation on electrical properties of *n*-type GaN surfaces

Takeshi Kimura[a] and Tamotsu Hashizume[b]
Research Center for Integrated Quantum Electronics (RCIQE) and Graduate School of Information Science and Technology, Hokkaido University, North-13 West-8, Kita-ku, Sapporo 060-8628, Japan

(Received 15 October 2008; accepted 18 November 2008; published online 6 January 2009)

We intentionally incorporated carbon into *n*-GaN by high-temperature annealing of a $SiN_x/CN_x/GaN$ structure to study the effect of unintentional carbon incorporation on the electrical properties of *n*-type GaN surfaces. X-ray photoelectron spectroscopy results showed outdiffusion of Ga atoms from the GaN surface during high-temperature annealing even when the SiN_x layer was present. The current-voltage characteristics showed a drastic increase in current in the forward and reverse directions of the Schottky diode in the carbon-incorporated sample. They also showed no temperature dependence from 150 to 300 K. The current-voltage curves of the carbon-incorporated samples in the forward and reverse directions could be almost completely reproduced by assuming an exponentially decaying distribution from the surface for shallow donors. © *2009 American Institute of Physics*. [DOI: 10.1063/1.3056395]

I. INTRODUCTION

Carbon and oxygen are impurities that may contaminate GaN-based devices when they are being fabricated. For example, the ion implantation technique is one of the most commonly used processes in semiconductor technology because it can introduce a well-defined impurity doping profile in the selected region. For GaN-based devices, however, high-temperature annealing (1 000–1 300 °C) is necessary for effective activation of impurities in the donor or acceptor state and for recovery from implantation-induced crystalline defects.[1–3] Even if one utilizes a protection layer on the GaN surface, high-temperature annealing processes will cause electrical degradation of the surface associated with the decomposition (such as out diffusion of Ga and/or N atom) and/or unintentional impurity (such as carbon and oxygen) incorporation.

In particular, carbon is known as amphoteric impurity in III-V semiconductors. In fact, the amphoteric behavior of carbon was reported for GaAs, AlAs, and InAs grown by molecular beam epitaxy (MBE).[4] On the analogy of *p*-type doping of GaAs with C, several works were devoted to dope carbon into GaN. Hirota *et al.*[5] reported that the binding energy of the substitutional C at the N site (C_N) was 203 meV in the carbon-doped GaN by an ion implantation or a gas phase diffusion using C_2H_6. However, the *p*-type conduction was not observed in both samples. Efforts to produce *p*-type GaN:C have had only limited success. The C doping during epitaxial growth of GaN typically produces a highly resistive layer,[6] except for the *p*-type conductivity in cubic-phase GaN grown on GaAs by rf-assisted MBE using electron-beam evaporation of graphite.[7] The difficulty of the *p*-type conduction by carbon in a wurtzite structure may be attributed to the fact that the formation energy of the C_N is not small on the surface of *p*-type material.[8] Moreover, on the Ga-terminated (0001) surface, the substitutional doping of carbon on the N site may not be efficient.[9] Thus, the amphoteric nature on the carbon-related levels in GaN seems to depend on the crystalline quality of GaN and the device processing condition. However, no study that we know of has reported on the influence of unintentional incorporation of carbon impurities into GaN during high-temperature annealing.

The purpose of this paper is to investigate the effect of carbon incorporation on the electrical properties of *n*-type GaN surfaces. To limit the study to the effect of carbon incorporation, we intentionally incorporated carbon into *n*-GaN by using high-temperature annealing of a $SiN_x/CN_x/GaN$ structure. A carbon-rich CN_x layer was utilized as the source, while SiN_x acted as a capping layer. By using the CN_x layer, we could artificially reproduce the situation in which carbon impurities are included in the SiN_x protection layer of actual device processes. Carbon incorporation was confirmed by secondary ion mass spectrometry (SIMS). The electrical properties of the carbon-incorporated GaN surface were studied by measuring temperature-dependent current-voltage (*I-V*) characteristics. As a result, the incorporated carbon behaves as a shallow donor with a binding energy of 30 ± 20 meV in GaN, which indicates the incorporated carbon mainly substitutes for the Ga. The observed lack of dependence on temperature of the *I-V* characteristics can be explained with the thin surface barrier (TSB) model.

II. EXPERIMENTAL

Figure 1(a) shows the flowchart of the carbon incorporation process in GaN. We used *n*-type GaN with Si doping of 1×10^{17} cm^{-3} grown on a sapphire substrate by metal-organic chemical vapor deposition. The GaN surface was cleaned in the electron-cyclotron-resonance (ECR)-excited N_2 plasma. We fabricated the $SiN_x/CN_x/GaN$ structure by ECR-CVD. A thin CN_x layer with a thickness of 2–10 nm

[a]Electronic mail: kimura@rciqe.hokudai.ac.jp.
[b]Electronic mail: hashi@rciqe.hokudai.ac.jp.

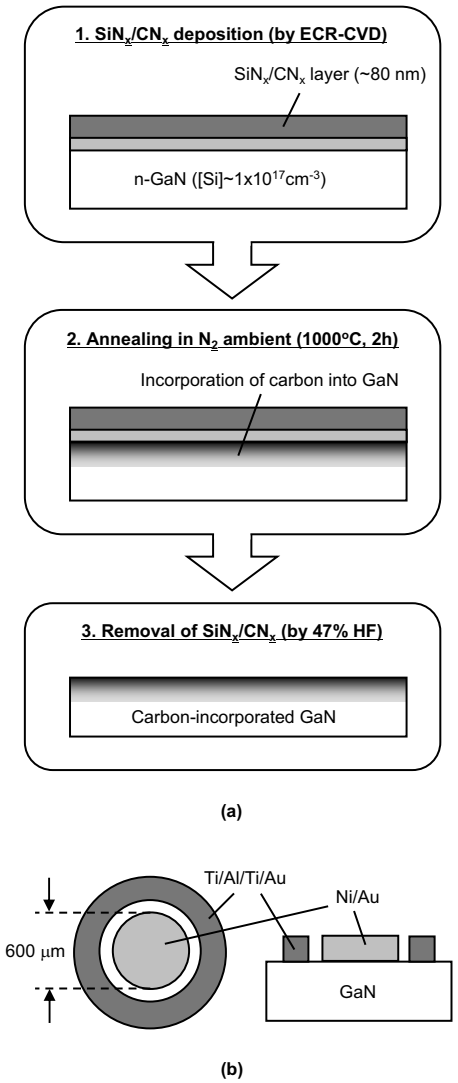

FIG. 1. (a) Flowchart of carbon incorporation process in GaN. (b) Sample structure of Schottky diode.

was deposited on the GaN surface at room temperature using a gas mixture of CH_4/N_2 as a source. In the subsequent *in situ* stage, the SiN_x layer was deposited at 260 °C using a gas mixture of SiH_4/N_2. Ellipsometry analysis showed that the thickness and the refractive index of SiN_x were 80 nm and 2.04, respectively. The sample was annealed at 1 000 °C for 120 min in a N_2 ambient to incorporate the carbon impurity into the GaN layer. The SiN_x/CN_x bilayer was then removed from the *n*-GaN surface in a 47% HF solution. After the carbon incorporation process, we fabricated circular Ni/Au Schottky diodes with Ti/Al/Ti/Au Ohmic ring electrodes, as shown in Fig. 1(b). Ni/Au Schottky contacts with a diameter of 600 μm were formed by electron-beam deposition. To remove the residual carbon on the GaN surface, we cleaned the GaN surface by using ECR-excited N_2 plasma before evaporating the metal contacts.

The chemical properties of the SiN_x and GaN surfaces were characterized using an x-ray photoelectron spectroscopy (XPS) system (ParkinElmer PHI 1600C) with a spherical capacitor and a monochromatic Al $K\alpha$ radiation source ($h\nu$=1486.6 eV). The energy scale was calibrated to the Au4f spectrum ($h\nu$=84.0 eV). The carbon density of the

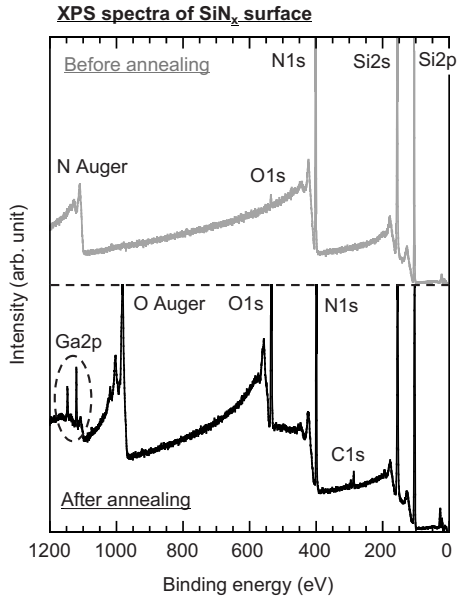

FIG. 2. Comparison of wide-scan XPS spectra of SiN_x surface before and after annealing.

GaN layer after the incorporation process was characterized using a SIMS system (PHI-6650, ULVAC-PHI Inc.). The temperature-dependent *I-V* characteristics of the Schottky diodes were measured in a BCT-21MDC semiconductor parameter low-temperature prober system (Nagase & Co., Ltd.) using an Agilent 4156C semiconductor parameter analyzer. For the carrier concentration measurement, we deposited a Ti/Al/Ti/Au multilayer on the corner of a square sample and annealed the sample in a N_2 ambient at 800 °C for 1 min.

III. RESULTS AND DISCUSSION

A. Ga outdiffusion and carbon incorporation during high-temperature annealing

Figure 2 compares the wide-scan XPS spectra of the SiN_x surface before and after high-temperature annealing. After annealing, the peaks corresponding to the Ga 2*p* level appeared in the XPS spectrum. This indicates the outdiffusion of Ga atoms to the SiN_x layer during the 1 000 °C annealing. Additionally, the full width at half maximum of the Ga 3*d* XPS spectrum after removing the SiN_x/CN_x bilayer from the annealed $SiN_x/CN_x/GaN$ structure became wider than the one from the virgin GaN surface, as shown in Fig. 3. This is also attributed to the decomposition of the GaN surface during the high-temperature annealing. Ga vacancies are known to have relatively low formation energies in *n*-type GaN;[10,11] thus, these characteristics indicate that Ga vacancies were generated by the high-temperature annealing.

The density profile of incorporated carbon in GaN was investigated using SIMS. Figure 4 shows SIMS profiles of carbon density for virgin and carbon-incorporated samples. The detection limit was determined by measuring the carbon density in an intentionally carbon-implanted GaN sample. The results in Fig. 4 clearly show the incorporation of carbon to a depth of 200–300 nm for the intentionally incorporated GaN sample.

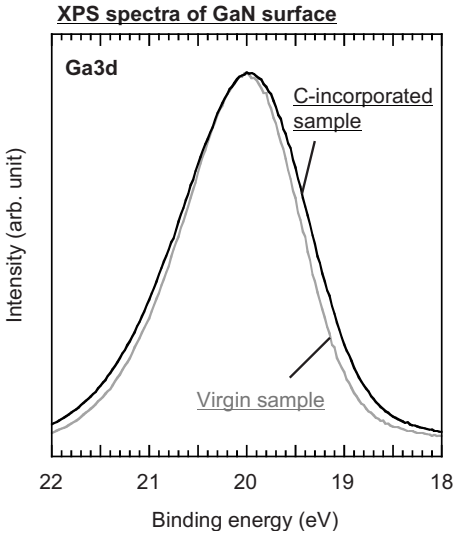

FIG. 3. Comparison of Ga 3*d* XPS spectra between virgin and carbon-incorporated GaN surfaces.

B. Temperature-dependent *I-V* characteristics of virgin and carbon-incorporated GaN Schottky diode

Figure 5 shows the temperature-dependent *I-V* characteristics of the virgin and carbon-incorporated samples. The carbon-incorporated sample showed a drastic increase in current in both forward and reverse directions. To confirm that this current increase was induced by the incorporated carbon, we compared the *I-V* characteristics of the carbon-incorporated sample with two other samples: one to confirm the influence of high-temperature annealing and the other to confirm the influence of the high-power plasma process in the deposition of the CN_x layer. We fabricated the SiN_x/GaN and CN_x/GaN structures by ECR-CVD. The SiN_x/GaN sample was annealed at 1 000 °C for 120 min in a N_2 ambient; then, the SiN_x layer was removed from the GaN surface in a 47% HF solution. The CN_x layer of the CN_x/GaN sample was removed without high-temperature annealing. The *I-V* characteristics of the Schottky diodes fabricated on

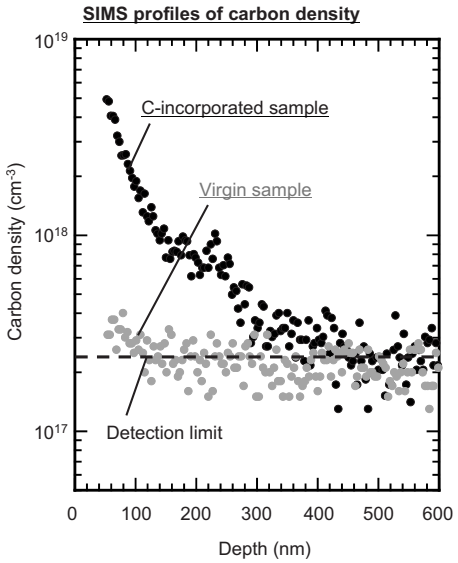

FIG. 4. SIMS profiles of carbon density for virgin and carbon-incorporated samples.

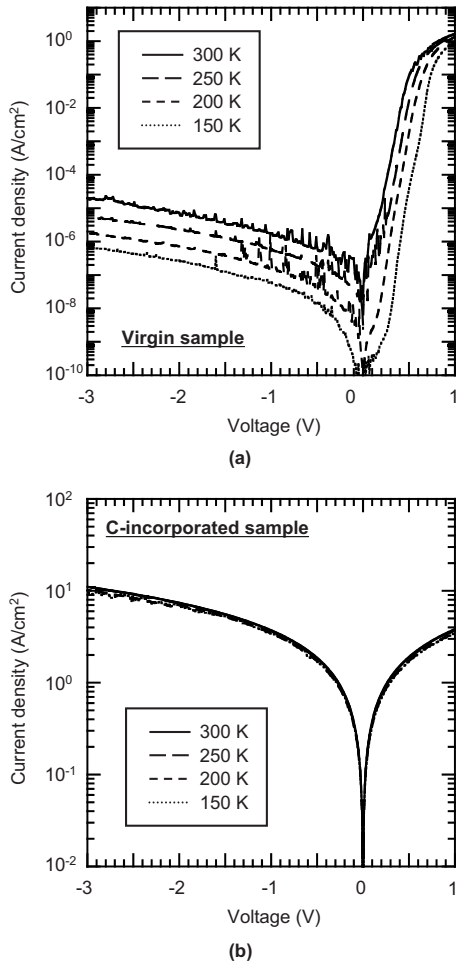

FIG. 5. Temperature-dependent *I-V* characteristics of (a) virgin sample and (b) carbon-incorporated sample.

both samples were similar to those of the virgin sample. Hence, the large increase in current of the Schottky diode was induced by incorporated carbon.

In addition, while the *I-V* characteristics of the virgin sample changed systematically with temperature, the *I-V* characteristics of the carbon-incorporated sample showed no temperature dependence from 150 to 300 K. This indicates thermionic emission (TE) is the dominant current transport process in the virgin sample. In the carbon-incorporated sample, on the other hand, thermionic field emission (TFE) or field emission (FE) is the major current leakage path in the forward and reverse directions.

C. Analysis of carbon-incorporated sample based on TSB model

Figure 6 schematically shows the energy band diagrams under the reverse bias condition and the carrier profiles. Figure 6(a) shows diagrams for the ideal metal/*n*-GaN Schottky junction, whereas Fig. 6(b) shows the case with surface donors. Hasegawa and co-workers[12,13] proposed the TSB model for forward and reverse current transport in GaN Schottky barriers. This model assumes that there are high-density donors near the Schottky interface; this reduces the width of the Schottky potential, thereby increasing the number of electrons tunneling through the thin surface barrier in both direc-

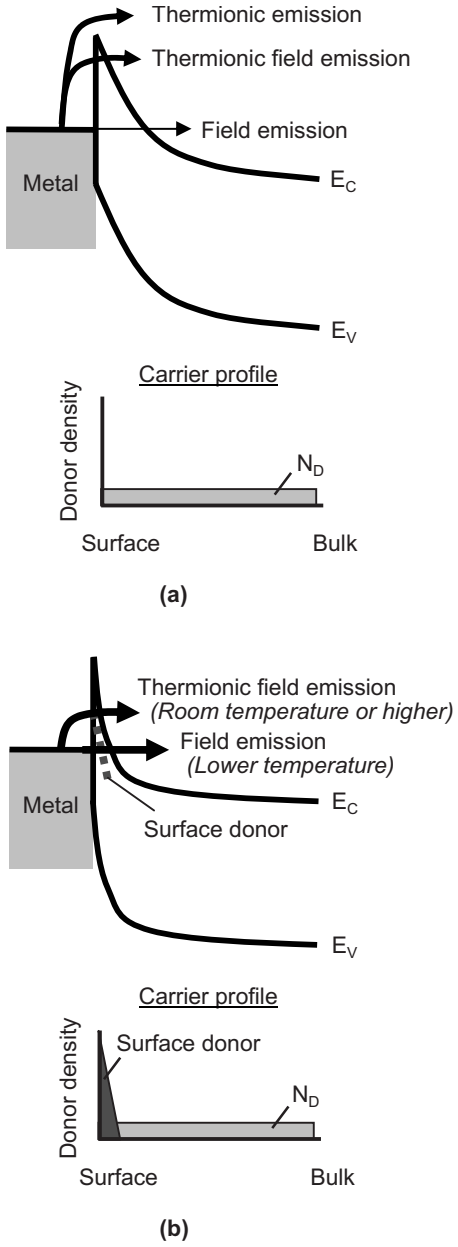

FIG. 6. Schematic illustrations of energy band diagram under the reverse bias condition and carrier profile for (a) the ideal metal/*n*-GaN Schottky junction and (b) the case with surface donors.

tions. Therefore, either the TFE or FE mechanism becomes dominant and reduces the temperature dependence. It is likely that the substitutional carbon at the Ga site behaves as a shallow donor with a binding energy of 30 meV in GaN,[5,14] and high-density substitutional C_{Ga} exists in the surface region; thus both forward and reverse currents in the carbon-incorporated sample would increase. If the incorporated carbon substituted for N, the substitutional C_N would behave as an acceptor and compensate for the donor. However, the experimental data showed no such phenomenon. One of the reasons is that while Ga vacancies are more favorable under *n*-type conditions, the formation energy of the N vacancy is large in *n*-type conditions.[10,11] Thus, there is a possibility that few N vacancies are generated during high-temperature annealing and that Ga vacancies are generated instead.

We tried to reproduce the experimental data by calculating the *I-V* characteristics based on the TSB model analysis

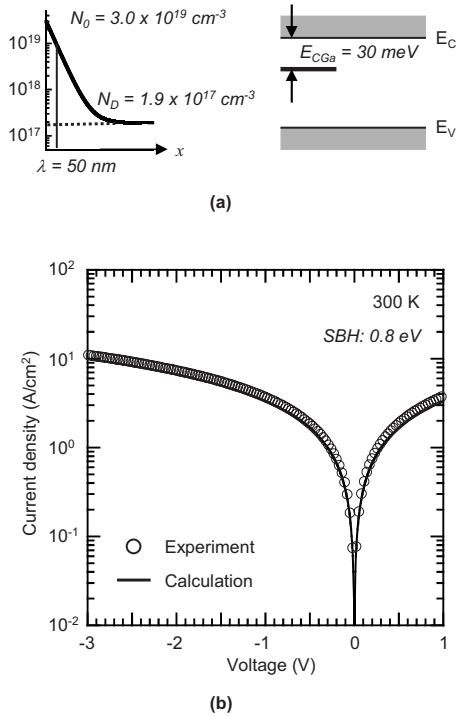

FIG. 7. (a) Best choice of distribution shape and parameter values to reproduce the experimental data of the carbon-incorporated sample. (b) Calculated *I-V* curves (solid curves) fitted to experimental data (symbols) of the carbon-incorporated sample.

of Kotani *et al.*[13] The substitutional C_{Ga} near the surface was assumed to have the following exponential distribution:

$$N_{CGa}(x) = N_0 \exp\left(-\frac{x}{\lambda}\right), \tag{1}$$

where x is depth from surface, N_0 is the peak density of C_{Ga} at the surface, and λ is decay constant. Another important parameter, the energy depth, E_{CGa}, of the substitutional C_{Ga} was varied as a fitting parameter. The bulk shallow donor density N_D was set to be that of the experimental sample of $N_D = 1.9 \times 10^{17}$ cm^{-3}. Hirota *et al.*[5] estimated the binding energy of the C donor level to be 30 meV (the substitutional C_{Ga}). Wang and Chen[14] also predicted the ionization energy of the C_{Ga} donor to be 34.0 meV from the calculation using the effective-mass approximation. In reference to these results, we used the value of 30 meV for the C donor level in our calculation to reproduce the experimental *I-V* data. Then, as shown in Fig. 7, we obtained the excellent fitting result for the carbon-incorporated GaN Schottky diode by assuming the exponentially decaying distribution shown in Fig. 7(a). The simulation almost completely reproduced the forward and reverse *I-V* behavior. In addition, the C_{Ga} distribution is similar to the carbon density profile obtained by SIMS in Fig. 4. From the separate calculation by changing the value of the energy level, we found that the accuracy of the energy level was 30 ± 20 meV. The calculated *I-V* characteristics for the virgin sample also reproduced the experimental data by using the same parameters of Schottky barrier height (SBH)=0.80 eV and $N_D = 1.9 \times 10^{17}$ cm^{-3} as the carbon-incorporated sample.

D. Two-layer Hall analysis of carbon-incorporated sample

Finally, we measured the change in carrier concentration of the GaN layer before and after the carbon incorporation process. The carrier concentration of the virgin *n*-GaN was 1.9×10^{17} cm^{-3}. After incorporation, it increased to 3.0×10^{17} cm^{-3}. However, this result is for the whole sample with a thickness of 3 μm consisting of an upper carbon-incorporated layer and a GaN under layer. Thus, we calculated the carrier concentration of only the upper carbon-incorporated layer by using two-layer Hall analysis.[15–17] The carrier concentration of upper carbon-incorporated layer, n_{ci}, is given as follows:

$$n_{ci} = \frac{1}{d_{ci}} \frac{(n\mu d - n_{GaN}\mu_{GaN}d_{GaN}t)^2}{n\mu^2 d - n_{GaN}\mu_{GaN}^2 d_{GaN}t}. \quad (2)$$

Here, n and n_{GaN} are the carrier concentrations of the whole sample and GaN under layer, μ and μ_{GaN} are the carrier mobilities of the whole sample and GaN under layer, d, d_{ci}, and d_{GaN} are the thicknesses of the whole sample, upper carbon-incorporated layer, and GaN under layer, and t is the correction factor related to the series resistance between the upper and under layers. The parameters of the GaN under layer were those of the virgin GaN results.

When the thickness of carbon-incorporated layer was taken from the SIMS profile to be 200 nm, the carrier concentration of the carbon-incorporated layer was calculated to be 2.4×10^{18} cm^{-3}. Even in this case, the carrier concentration near the surface (~50 nm), which has more of an effect on the Schottky contact, was estimated to be 1.0×10^{19} cm^{-3}. This value is consistent with the SIMS results (Fig. 4) and the assumed carrier profile [Fig. 7(a)]. Such high-density shallow donors (incorporated carbon) will reduce the width of the Schottky potential and increase the tunneling currents through the Schottky barrier. In relation to the increase in carrier concentration near the surface after the carbon incorporation, we observed a slight decrease in the sheet resistivity for the present sample. When we used an undoped *n*-type GaN layer with a different thickness, the sheet resistivity was found to increase slightly.[18] This discrepancy may arise from the difference of crystalline quality among the GaN layers. In the undoped GaN layer, it is likely that the *n*-type conduction originates from the existence of nitrogen vacancies or oxygen impurities. In this case, there is a possibility that the incorporated carbon can form deep levels in complex configuration with such residual defects or impurities. This may result in a partial compensation of the residual donors in undoped GaN, leading to the slight increase in resistivity.

IV. CONCLUSIONS

We intentionally incorporated carbon into *n*-GaN by using high-temperature annealing of a $SiN_x/CN_x/GaN$ structure to study the effect of unintentional incorporation of carbon on the electrical properties of *n*-type GaN. The main conclusions are as follows.

(1) The XPS results showed out diffusion of Ga atoms from the GaN surface during high-temperature annealing even when the SiN_x layer existed.
(2) The SIMS results clearly showed incorporation of carbon into GaN to a depth of 200–300 nm.
(3) The *I-V* characteristics showed a drastic increase in current in the forward and reverse directions of the Schottky diode in the carbon-incorporated sample. They also showed no temperature dependence from 150 to 300 K.
(4) The measured *I-V* curves of the carbon-incorporated sample could be almost completely reproduced in the forward and reverse directions by assuming an exponentially decaying distribution from the surface for the shallow donors with an energy depth of 30 meV.
(5) The carbon incorporated during the high-temperature annealing mainly substituted for Ga, and this substitutional C_{Ga} behaved as a shallow donor in GaN, leading to a high-density doping effect near the GaN surface. This reduced the width of the Schottky potential, allowing electrons to tunnel thorough the thin barrier.

In conclusion, unintentional incorporation of carbon impurities during GaN device fabrication process may induce current leaks in Schottky contacts. Therefore, the device should be carefully made so that the actual device process does not unintentionally incorporate carbon.

ACKNOWLEDGMENTS

One of the authors (T.K.) would like to thank the Japan Society for the Promotion of Science (JSPS) Research Fellowships for Young Scientists.

[1] H. T. Wang, L. S. Tan, and E. F. Chor, Thin Solid Films **515**, 4476 (2007).
[2] K. Nomoto, T. Tajima, T. Mishima, M. Satoh, and T. Nakamura, IEEE Electron Device Lett. **28**, 939 (2007).
[3] D. Ozaki, J. Ebihara, Y. Ohshima, R. Takeuchi, and T. Inada, Nucl. Instrum. Methods Phys. Res. B **257**, 320 (2007).
[4] H. Ito and T. Ishibashi, Jpn. J. Appl. Phys., Part 2 **30**, L944 (1991).
[5] R. Hirota, K. Kushida, J. Takahashi, and K. Kuriyama, Nucl. Instrum. Methods Phys. Res. B **219**, 792 (2004).
[6] A. Armstrong, C. Poblenz, D. S. Green, U. K. Mishra, J. S. Speck, and S. A. Ringel, Appl. Phys. Lett. **88**, 082114 (2006).
[7] D. J. As, U. Kohler, M. Lubbers, J. Mimkes, and K. Lischka, Phys. Status Solidi A **188**, 699 (2001).
[8] C. H. Seager, A. F. Wright, J. Yu, and W. Gotz, J. Appl. Phys. **92**, 6553 (2002).
[9] T. Hikosaka, T. Narita, Y. Honda, M. Yamaguchi, and N. Sawaki, Appl. Phys. Lett. **84**, 4717 (2004).
[10] S. Limpijumnong and C. G. Van de Walle, Phys. Rev. B **69**, 035207 (2004).
[11] M. A. Reshchikov and H. Morkoc, J. Appl. Phys. **97**, 061301 (2005).
[12] H. Hasegawa and S. Oyama, J. Vac. Sci. Technol. B **20**, 1647 (2002).
[13] J. Kotani, T. Hashizume, and H. Hasegawa, J. Vac. Sci. Technol. B **22**, 2179 (2004).
[14] H. Wang and A.-B. Chen, J. Appl. Phys. **87**, 7859 (2000).
[15] R. L. Petritz, Phys. Rev. **110**, 1254 (1958).
[16] D. C. Look, C. E. Stutz, and C. A. Bozada, J. Appl. Phys. **74**, 311 (1993).
[17] B. Arnaudov, T. Paskova, S. Evtimova, E. Valcheva, M. Heuken, and B. Monemar, Phys. Rev. B **67**, 045314 (2003).
[18] T. Kimura, S. Ootomo, T. Nomura, S. Yoshida, and T. Hashizume, Jpn. J. Appl. Phys., Part 2 **46**, L224 (2007).